2 Ray optics

If one shines a laser beam on a large transparent object, such as the prism shown in Fig. 2.1, a fraction of the power of the beam will be reflected back and the rest will go through and exit from the other side. Because the directions of the reflected and transmitted beams are different from that of the incoming beam, the mechanical momentum associated with the light beam changes and, by Newton's action–reaction law, a force acts on the object. As long as one deals with objects that are much larger than the wavelength of light, which is typically around one micrometre for optical tweezing applications, the behaviour of the laser beam can be accurately described by considering it as a collection of *light rays* and employing the tools of *geometrical optics*. One can also make use of geometrical optics for the calculation of optical forces and obtain accurate results when dealing with relatively large objects, such as cells and large colloidal particles, whose size is typically significantly larger than one micrometre. In this chapter, we will therefore study optical forces using the geometrical optics approach, as this permits us to introduce in a more intuitive way many concepts that give insight into the mechanism by which microscopic particles can be optically trapped and that will be treated more rigorously in Chapters 3, 5 and 6.

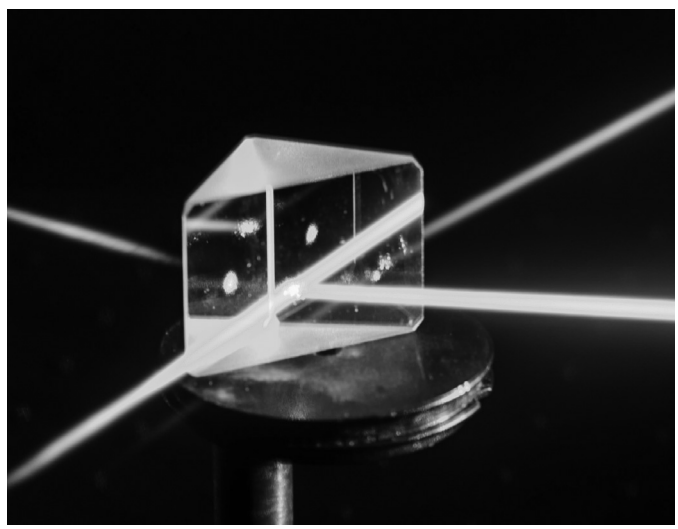

Figure 2.1 Reflection and transmission on a prism. As a laser light beam impinges on a prism, it is partly reflected and partly transmitted. The directions of the reflected and transmitted beams are different from that of the incoming beam. This change of direction entails a change of the momentum associated with the light beam and, because of the action–reaction law, a force acting on the prism. Picture credits: Marco Grasso and Alessandro Magazzù.

https://doi.org/10.1017/CBO9781107279711.004 Published online by Cambridge University Press

2.1 Optical rays

The density of the energy flux due to an electromagnetic wave is given by the Poynting vector $\mathbf{S}$ or, equivalently, by the number of photons passing through a unit area per unit time multiplied by the energy per photon.[1] In order to describe how this energy is transported, a series of rays can be associated with an electromagnetic wave. These rays are lines perpendicular to the electromagnetic wavefronts and pointing in the direction of the electromagnetic energy flow, i.e., the direction of $\mathbf{S}$. For example, Fig. 2.2 shows the rays associated with a plane electromagnetic wave constructed by dividing the wavefront into several portions of equal area A and by associating with each of these portions a ray with power

$$P = |\mathbf{S}|A. \tag{2.1}$$

When a light ray $\mathbf{r}_\mathrm{i}$ impinges on a flat surface between two media with different optical impedances, or *refractive indices*, part of it is reflected and part transmitted, as shown in Fig. 2.3. The *angle of incidence* θ_i is the angle between $\mathbf{r}_\mathrm{i}$ and the line n normal to the surface at the incidence point. For the *angle of reflection* θ_r, the law of reflection

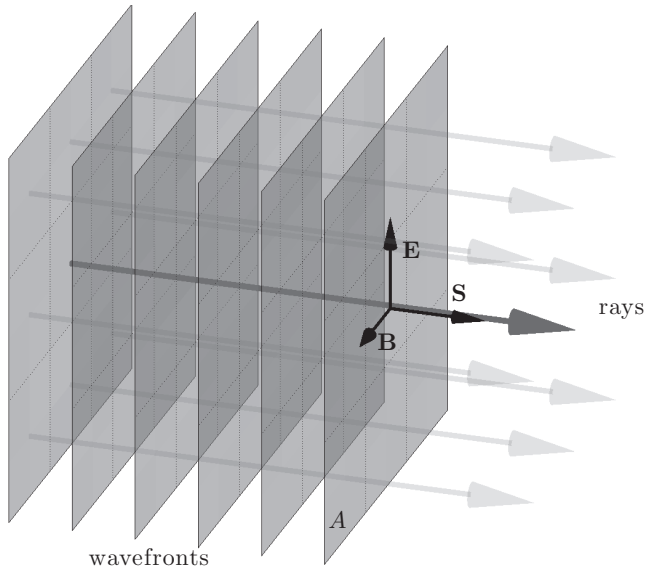

Figure 2.2 From electromagnetic waves to rays. Optical rays (grey arrows) are perpendicular to the wavefronts of an electromagnetic wave (planes) and parallel to the Poynting vector ($\mathbf{S}$).

[1] Here, and in the rest of this chapter, we are implicitly considering a monochromatic electromagnetic wave. In terms of the physical fields $\boldsymbol{\mathcal{E}}(\mathbf{r}, t)$ and $\boldsymbol{\mathcal{B}}(\mathbf{r}, t)$, $\mathbf{S} = \overline{\boldsymbol{\mathcal{S}}} = \frac{1}{\mu}\overline{\boldsymbol{\mathcal{E}} \times \boldsymbol{\mathcal{B}}}$ [Box 3.6]. In terms of the phasors $\mathbf{E}(\mathbf{r})$ and $\mathbf{B}(\mathbf{r})$ [Box 3.5], $\mathbf{S} = \frac{1}{2\mu}\mathrm{Re}\{\mathbf{E} \times \mathbf{B}^*\}$ [Box 3.6].

https://doi.org/10.1017/CBO9781107279711.004 Published online by Cambridge University Press

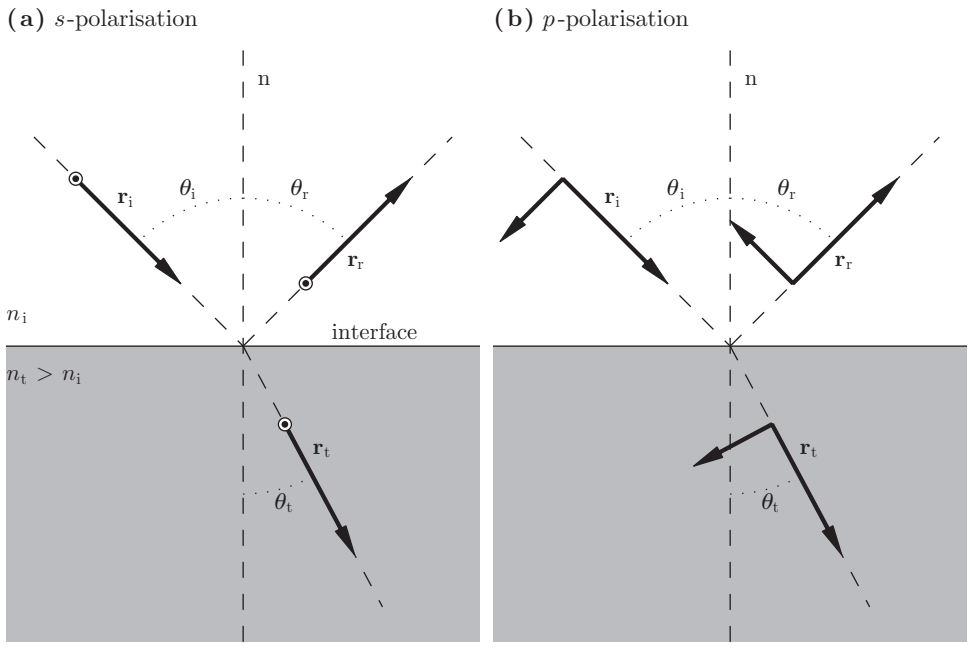

Figure 2.3 Reflection and transmission at a planar interface. As (a) an s-polarised or (b) a p-polarised ray $\mathbf{r}_\mathrm{i}$ impinges on a planar interface between two media with refractive indices n_i and n_t, it splits into a reflected ray $\mathbf{r}_\mathrm{r}$ and a transmitted ray $\mathbf{r}_\mathrm{t}$. The arrows perpendicular to the rays represent the directions of the electric fields, and n is the line perpendicular to the interface at the incidence point.

states that

$$\theta_\mathrm{r} = \theta_\mathrm{i}, \tag{2.2}$$

and for the *angle of transmission* θ_t, Snell's law states that

$$n_\mathrm{t} \sin\theta_\mathrm{t} = n_\mathrm{i} \sin\theta_\mathrm{i}, \tag{2.3}$$

where n_i is the refractive index of the medium in which the incident ray propagates and n_t is that of the medium in which the transmitted ray propagates. Both the reflected and transmitted rays are contained in the *plane of incidence*, i.e., the plane that contains $\mathbf{r}_\mathrm{i}$ and n.

As a consequence of energy conservation, the incoming power P_i must be equal to the sum of the reflected power P_r and the transmitted power P_t; i.e.,

$$P_\mathrm{i} = P_\mathrm{r} + P_\mathrm{t}. \tag{2.4}$$

How the power is split between the reflected and transmitted rays can be calculated using Maxwell's laws [Box 3.1] by imposing continuity across the interface of the tangential

https://doi.org/10.1017/CBO9781107279711.004 Published online by Cambridge University Press

components of the electric and magnetic fields [Box 3.2]. The result depends on the polarisation of the incoming ray and is expressed by *Fresnel's equations*. For s-polarised light, i.e., light whose electric field vector is normal to the plane of incidence [Fig. 2.3a], the intensity reflection coefficient is given by

$$R_s = \left| \frac{n_\mathrm{i} \cos\theta_\mathrm{i} - n_\mathrm{t} \cos\theta_\mathrm{t}}{n_\mathrm{i} \cos\theta_\mathrm{i} + n_\mathrm{t} \cos\theta_\mathrm{t}} \right|^2 \tag{2.5}$$

and the intensity transmission coefficient by

$$T_s = \frac{4 n_\mathrm{i} n_\mathrm{t} \cos\theta_\mathrm{i} \cos\theta_\mathrm{t}}{|n_\mathrm{i} \cos\theta_\mathrm{i} + n_\mathrm{t} \cos\theta_\mathrm{t}|^2}. \tag{2.6}$$

For p-polarised light, i.e., light whose electric field vector is contained in the plane of incidence [Fig. 2.3b], the intensity reflection coefficient is given by

$$R_p = \left| \frac{n_\mathrm{i} \cos\theta_\mathrm{t} - n_\mathrm{t} \cos\theta_\mathrm{i}}{n_\mathrm{i} \cos\theta_\mathrm{t} + n_\mathrm{t} \cos\theta_\mathrm{i}} \right|^2 \tag{2.7}$$

and the intensity transmission coefficient by

$$T_p = \frac{4 n_\mathrm{i} n_\mathrm{t} \cos\theta_\mathrm{i} \cos\theta_\mathrm{t}}{|n_\mathrm{i} \cos\theta_\mathrm{t} + n_\mathrm{t} \cos\theta_\mathrm{i}|^2}. \tag{2.8}$$

It is straightforward to verify that $R_s + T_s = 1$ and $R_p + T_p = 1$, fulfilling the energy conservation statement in Eq. (2.4). For unpolarised or circularly polarised light, one can use the average of the previous coefficients, obtaining

$$R = \frac{R_s + R_p}{2} \tag{2.9}$$

and

$$T = \frac{T_s + T_p}{2}. \tag{2.10}$$

To keep the discussion simple, in the rest of this chapter we will consider all rays to be circularly polarised, unless otherwise stated.

https://doi.org/10.1017/CBO9781107279711.004 Published online by Cambridge University Press

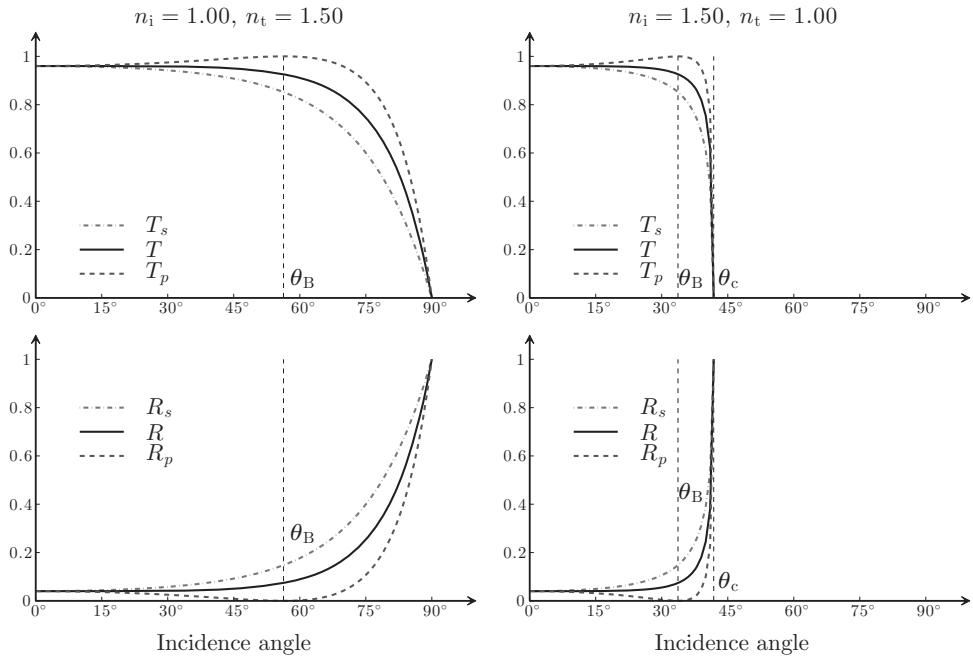

Figure 2.4 Fresnel's coefficients. Fresnel's transmission and reflection coefficients for a ray going from air to glass (left) and from glass to air (right). θ_B and θ_c are Brewster's angle and the critical angle, respectively.

The values of the reflection and transmission coefficients are plotted in Fig. 2.4. For an s-polarised wave the transmission efficiency decreases monotonically as θ_i increases, whereas for a p-polarised wave the transmission efficiency first increases until all incident light is transmitted at *Brewster's angle*,

$$\theta_B = \arctan\left(\frac{n_t}{n_i}\right), \tag{2.11}$$

and then decreases. Going from a medium with a lower refractive index, e.g., air ($n_m = 1.00$), to a medium with higher refractive index, e.g., glass ($n_m = 1.50$), there is always transmission; this is not the case in the opposite direction, e.g., going from glass to water, because above the *critical angle*

$$\theta_c = \arcsin\left(\frac{n_t}{n_i}\right) \tag{2.12}$$

both s-polarised and p-polarised light are completely reflected; this phenomenon is known as *total internal reflection*.

Exercise 2.1.1 Derive Fresnel's equations [Eqs. (2.5), (2.6), (2.7) and (2.8)]. [Hint: Use Maxwell's laws [Box 3.2] and impose continuity across the interface of the tangential components of the electric and magnetic fields [Box 3.4].]

https://doi.org/10.1017/CBO9781107279711.004 Published online by Cambridge University Press

2.2 Optical forces

A photon, i.e., a particle representing a quantum of light, of wavelength λ_0 in vacuum carries energy $u = hc/\lambda_0$, where h is the Planck constant and c is the speed of light in vacuum, and momentum $\mathbf{p} = (h/\lambda_0)\hat{\mathbf{u}}$, where $\hat{\mathbf{u}}$ is a unit vector indicating the photon's direction of motion. When such a photon is elastically scattered by an object, its energy does not change, but its momentum can change direction, resulting in a recoil force acting on the object.

A light ray with power P carries $N = P/u$ photons per second past a fixed point. If, as shown in Fig. 2.5a, such a ray impinges with normal incidence on a mirror, it will be completely reflected back, so that the momentum of each photon changes by $-2\mathbf{p}$ and the total change of momentum per unit time of the ray is $-2N\mathbf{p} = -2(P/c)\hat{\mathbf{u}}$. Thus, by Newton's action–reaction law, the recoil force on the mirror is

$$\mathbf{F}_{\text{reflection}} = \frac{2P}{c}\hat{\mathbf{u}}, \tag{2.13}$$

which is, in fact, the maximum optical force that can be generated by a ray (or a laser beam) of power P. For example, for a 1 mW laser beam, Eq. (2.13) gives a force of just 7×10^{-12} N, i.e., 7 piconewtons. Although small, this force is comparable to the forces that are relevant in the microscopic and nanoscopic world, e.g., the forces generated by molecular motors, and gives us a first impression of the potential of optical manipulation.

In general, as shown in Fig. 2.5b, a ray will impinge with *non-normal* incidence on a *non-planar* surface and will be partly reflected and partly transmitted. Thus, in order to calculate the forces associated with the reflection and transmission of a ray $\mathbf{r}_\text{i}$ of power P_i in direction $\hat{\mathbf{r}}_\text{i}$, one typically needs to

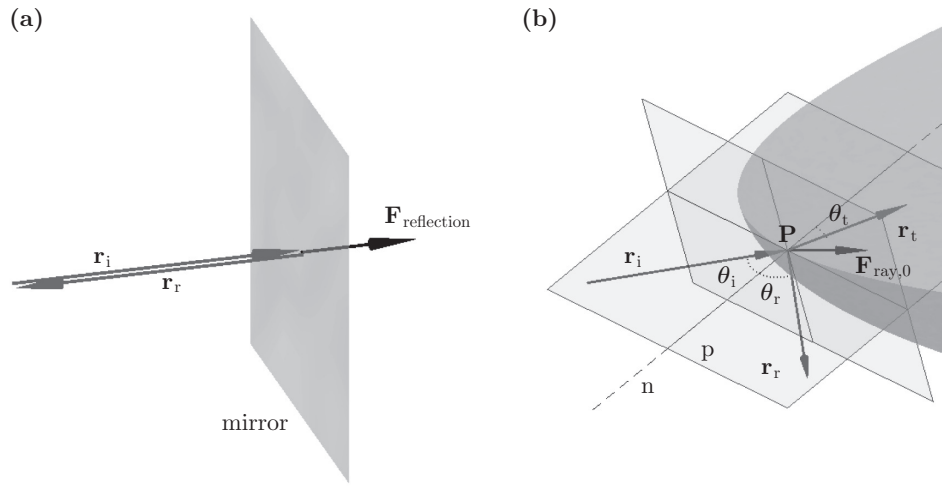

Figure 2.5 Ray optics forces: (a) Force generated by the reflection of a light ray impinging with normal incidence on a mirror. (b) Force generated by the scattering of a light ray by a generic surface with a generic angle of incidence.

https://doi.org/10.1017/CBO9781107279711.004 Published online by Cambridge University Press

Box 2.1 What is the momentum of light?

What happens to the momentum of a photon when it enters a material medium? Hermann Minkowski (1908) considered that the momentum p carried by a photon is inversely proportional to its wavelength λ_0; therefore, because in a medium of refractive index n the wavelength becomes λ_0/n, the photon momentum must *increase* by a factor n, i.e.,

$$p_{\mathrm{M}} = n\frac{h}{\lambda_0}.$$

One year later, Max Abraham (1909) argued that the momentum of an object is proportional to its velocity; therefore, because the speed of a photon in a medium becomes c/n, the photon momentum must *decrease* by a factor n, i.e.,

$$p_{\mathrm{A}} = \frac{1}{n}\frac{h}{\lambda_0}.$$

Since the beginning of the twentieth century, scientists' opinions on this matter have been swinging between the two positions, leading to the well-known *Abraham–Minkowski dilemma*. Pfeifer et al. (2007) provide an extensive review of this topic.

Experimental evidence in favour of either argument has been inconclusive, because most experiments measure the difference of the momentum carried by a beam before and after the interaction with an object and, because these momenta are calculated in the same medium, the Abraham–Minkowski dilemma does not produce any qualitative difference in the forces. A possibility would be to study what happens at an interface illuminated by a laser beam. Such an experiment was attempted by Ashkin and Dziedzic (1973): they showed that a narrow light beam impinging on a air–water interface produces an outward pull, resulting in the water surface bulging outward; consistent with the sign of the change of the Minkowski momentum, the bulge would be the result of the increased light momentum in water. However, it was later shown that this effect is governed by a radial gradient force – the water tends to collect in the high-intensity region of the laser beam, therefore the bulge – and that it provides no information on the longitudinal force associated with the linear momentum of light. So far, this and similar experiments have proved inconclusive.

A possible solution of this issue has been recently put forward by Stephen Barnett (2010). Surprisingly, both arguments would be reasonable and sound because they could be both right – but they refer to two different momenta, namely the *kinetic momentum*, where Abraham's theory is concerned, and the *canonical momentum*, where Minkowski's theory is concerned. These two momenta are actually the same when light is propagating in vacuum, but they can differ significantly in a medium.

1. find the incidence point **P** where the ray meets the surface, and the normal line n, which is perpendicular to the surface at **P**;
2. find the incidence plane p, i.e., the plane containing $\mathbf{r}_{\mathrm{i}}$ and n;
3. calculate the angle of incidence θ_{i}, i.e., the angle between $\mathbf{r}_{\mathrm{i}}$ and n, and derive θ_{r} and θ_{t} using Eqs. (2.2) and (2.3);
4. determine the directions $\hat{\mathbf{r}}_{\mathrm{r}}$ and $\hat{\mathbf{r}}_{\mathrm{t}}$ of the reflected ray $\mathbf{r}_{\mathrm{r}}$ and the transmitted ray $\mathbf{r}_{\mathrm{t}}$, which are contained in p;

https://doi.org/10.1017/CBO9781107279711.004 Published online by Cambridge University Press

5. calculate the power P_r and P_t of $\mathbf{r}_r$ and $\mathbf{r}_t$, respectively, using Fresnel's equations [Eqs. (2.5), (2.6), (2.7) and (2.8)] and taking into account the polarisation of the incoming ray;
6. calculate the force exerted on the object to which the surface belongs as

$$\mathbf{F}_{\text{ray},0} = \frac{n_i P_i}{c}\hat{\mathbf{r}}_i - \frac{n_i P_r}{c}\hat{\mathbf{r}}_r - \frac{n_t P_t}{c}\hat{\mathbf{r}}_t, \tag{2.14}$$

where the Minkowski momentum of light in a medium has been used.[2]

In general, if more than one ray interacts with an object, the total force is given by the sum of the forces generated by the reflection and transmission of each ray. In a similar way, it is also possible to consider the mechanical effects produced by the subsequent reflections and transmissions when the rays reach the surface of the object again.

Exercise 2.2.1 Show that the Abraham momentum of a ray of power P is P/c in every medium. How does Eq. (2.14) change when the Abraham momentum is used instead of the Minkowski momentum?

Exercise 2.2.2 Study numerically the force generated by the scattering of a ray at a planar interface as a function of the parameters of the system, e.g., angle of incidence and refractive indices of the media. Assume the ray to be circularly polarised.

Exercise 2.2.3 How do the optical forces due to the scattering of a ray on a planar surface change as a function of the polarisation of the ray?

2.3 Scattering and gradient forces

To understand the forces that act on a trapped microscopic particle, we start with a minimalistic model: the force due to a single ray $\mathbf{r}_i$ of power P_i hitting a dielectric sphere at an angle of incidence θ_i, as shown in Fig. 2.6a. As soon as $\mathbf{r}_i$ hits the sphere, a small amount of power is diverted into the reflected ray $\mathbf{r}_{r,0}$, while most of its power is carried by the transmitted ray $\mathbf{r}_{t,0}$. The ray $\mathbf{r}_{t,0}$ crosses the sphere until it reaches the opposite surface, where again it will be largely transmitted outside the sphere into the ray $\mathbf{r}_{t,1}$, while a small amount will be reflected inside the sphere into the ray $\mathbf{r}_{r,1}$. The ray $\mathbf{r}_{r,1}$ undergoes another scattering event as soon as it reaches the sphere boundary, and the process continues until all light has escaped from the sphere.[3] Repeatedly using Eq. (2.14) at each scattering event,

[2] The definition of the momentum of light in a medium is a very complex issue, which goes under the name of the *Abraham–Minkowski dilemma* and is still being debated. The Abraham and Minkowski definitions are equivalent in vacuum. In this book, we will consistently adopt the Minkowski momentum, in agreement with a large part of the optical manipulation literature. For a particle in a homogeneous medium of refractive index n_i, the alternative adoption of the Abraham form would generate forces smaller by a factor of n_i. Some further details are provided in Box 2.1.

[3] Although this is an asymptotic process that requires an infinite number of scattering events, typically virtually all light has escaped from the sphere within less than about 10 scattering events.

https://doi.org/10.1017/CBO9781107279711.004 Published online by Cambridge University Press

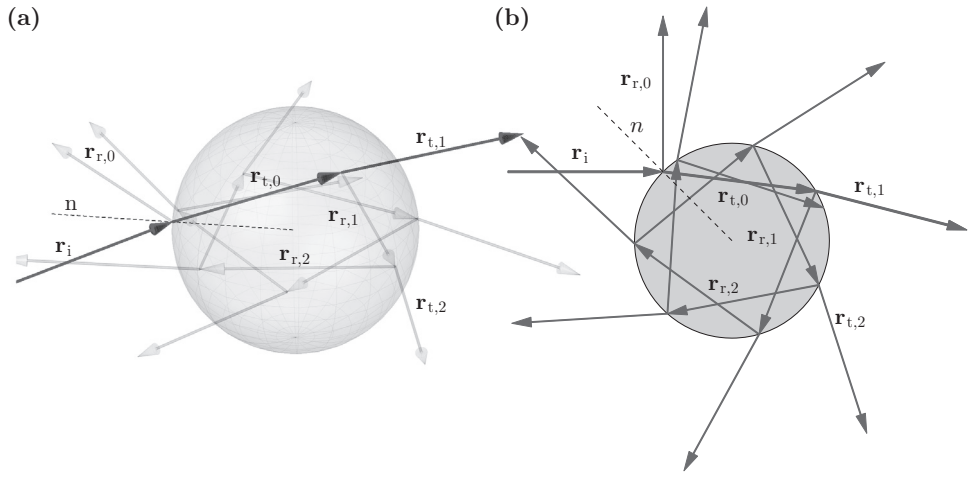

Figure 2.6 Scattering of a ray on a sphere. Multiple scattering of a light ray impinging on a sphere visualised (a) in three dimensions and (b) in the plane of incidence. Note how all the reflected and transmitted rays, as well as the vector of the force acting on the sphere (not shown), are contained in the plane of incidence.

it is possible to calculate the total force acting on the sphere as

$$\mathbf{F}_{\text{ray}} = \frac{n_i P_i}{c}\hat{\mathbf{r}}_i - \frac{n_i P_r}{c}\hat{\mathbf{r}}_{r,0} - \sum_{n=1}^{+\infty}\frac{n_i P_{t,n}}{c}\hat{\mathbf{r}}_{t,n}, \tag{2.15}$$

where $\hat{\mathbf{r}}_i$, $\hat{\mathbf{r}}_{r,n}$ and $\hat{\mathbf{r}}_{t,n}$ are unit vectors representing the direction of the incident ray and the nth reflected and transmitted rays, respectively. We can also notice that the definition of the momentum of the light beam inside the sphere [Box 2.1] does not matter for the final calculation; this is generally true for virtually all experiments involving optical forces.

Because, as shown in Fig. 2.6b, all the reflected and transmitted rays are contained in the plane of incidence, the force $\mathbf{F}_{\text{ray}}$ also has only components in the plane of incidence. In particular, it is possible to split $\mathbf{F}_{\text{ray}}$ into the optical *scattering force* $\mathbf{F}_{\text{ray,s}}$ that pushes the particle in the direction of the incoming ray ($\hat{\mathbf{r}}_i$) and the optical *gradient force* $\mathrm{F}_{\text{ray,g}}$ that pulls the particle in a direction perpendicular to that of the incoming ray ($\hat{\mathbf{r}}_\perp$); i.e.,

$$\mathbf{F}_{\text{ray}} = \mathbf{F}_{\text{ray,s}} + \mathbf{F}_{\text{ray,g}} = F_{\text{ray,s}}\hat{\mathbf{r}}_i + F_{\text{ray,g}}\hat{\mathbf{r}}_\perp. \tag{2.16}$$

Dividing $F_{\text{ray,s}}$ and $F_{\text{ray,g}}$ by $n_i P_i/c$, it is possible to define the dimensionless quantities known as the *trapping efficiencies* associated with the scattering and gradient forces, i.e.,

$$Q_{\text{ray,s}} = \frac{c}{n_i P_i}F_{\text{ray,s}}, \tag{2.17}$$

$$Q_{\text{ray,g}} = \frac{c}{n_i P_i}F_{\text{ray,g}}, \tag{2.18}$$

and the total trapping efficiency as their quadrature sum,

$$Q_{\text{ray}} = \sqrt{Q_{\text{ray,s}}^2 + Q_{\text{ray,g}}^2}. \tag{2.19}$$

https://doi.org/10.1017/CBO9781107279711.004 Published online by Cambridge University Press

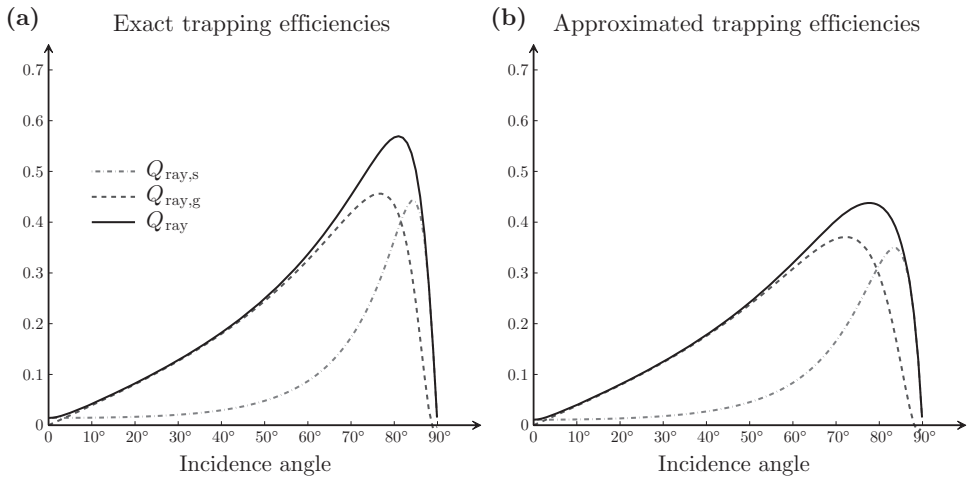

Figure 2.7 Trapping efficiencies for a glass ($n_{\text{p}} = 1.50$) spherical particle in water ($n_{\text{m}} = 1.33$) (a) taking into account all scattering events and (b) considering only the first two scattering events.

The trapping efficiencies permit one to quantify how effectively momentum is transferred from the light ray to the particle. From Eq. (2.13), we can see that the maximum value that they can reach is 2, corresponding to complete reflection of a ray at normal incidence. Fig. 2.7a shows the trapping efficiencies for a glass sphere in water; these reach up to 30% of their theoretical maximum value. $Q_{\text{ray,g}}$ grows much faster than $Q_{\text{ray,s}}$ as the angle of incidence increases, and the maximum efficiencies are obtained for relatively large angles of incidence ($\approx 80^\circ$). It is interesting to note that these results are independent of the size of the sphere.

Most of the contributions to the optical forces are due to the first two scattering events, i.e., the first reflection of the incoming beam and the first transmission out of the sphere. Fig. 2.7b shows that by calculating the scattering efficiencies accounting only for these two events one obtains a good approximation to the exact results presented in Fig. 2.7a, especially for small angles of incidence. This observation can be very useful in simplifying the numerical calculation of optical forces using ray optics in order to achieve high computational efficiency.

Exercise 2.3.1 Study how the trapping efficiencies $Q_{\text{ray,s}}$ [Eq. (2.17)], $Q_{\text{ray,g}}$ [Eq. (2.18)] and Q_{ray} [Eq. (2.19)] depend on the refractive index of the particle – e.g., silica ($n_{\text{p}} = 1.42$), polystyrene ($n_{\text{p}} = 1.49$), melamine ($n_{\text{p}} = 1.60$) and air bubble ($n_{\text{p}} = 1.00$) – and the medium – e.g., air ($n_{\text{m}} = 1.00$), water ($n_{\text{m}} = 1.33$) and immersion oil ($n_{\text{m}} = 1.50$). What happens when the refractive index of the particle is lower than that of the medium? How do these results depend on the polarisation of the incoming beam? [Hint: You can use the program `spscattering` from the book website.]

Exercise 2.3.2 Study how the trapping efficiencies depend on the number of scattering events that are considered for various combinations of refractive indices of the particle and

https://doi.org/10.1017/CBO9781107279711.004 Published online by Cambridge University Press

of the medium. [Hint: You can adapt the program `spscattering` from the book website.]

Exercise 2.3.3 Demonstrate that, when a ray is scattered by a sphere, all transmitted and reflected rays are contained in the incidence plane. Show that the optical forces are independent of the sphere size. [Hint: Read the original article by Ashkin (1992) studying optical forces on a sphere using geometrical optics.]

Exercise 2.3.4 Ashkin (1992) derived the following theoretical formulas for the scattering efficiencies of a circularly polarised ray on a sphere with angle of incidence θ_i:

$$Q_{\text{ray,s}} = 1 + R\cos 2\theta_i - T^2 \frac{\cos(2\theta_i - 2\theta_t) + R\cos 2\theta_i}{1 + R^2 + 2R\cos 2\theta_t}$$

and

$$Q_{\text{ray,g}} = R\sin 2\theta_i - T^2 \frac{\sin(2\theta_i - 2\theta_t) + R\sin 2\theta_i}{1 + R^2 + 2R\cos 2\theta_t},$$

where R and T are Fresnel's reflection and transmission coefficients and θ_t is the angle of transmission of the incident beam into the sphere. Show that some small corrections to these formulas are needed because of the change of the polarisation of the beam after the first scattering event. [Hint: You can adapt the program `spscattering` from the book website to compare the results of these formulas with the results obtained for the case of a circularly polarised ray.]

Exercise 2.3.5 Show that the gradient force that a ray exerts on a sphere is *conservative*, whereas the scattering force is *non-conservative*. What can you conclude for the force generated by a set of rays? [Hint: Use the definition of conservative force and line integrals.]

2.4 Counter-propagating beam optical trap

It is not possible to achieve stable trapping using a single ray because the particle is permanently pushed by the scattering force in the direction of the incoming ray. This is shown in Fig. 2.8a: a homogenous particle with refractive index higher than the surrounding medium, in this case a glass sphere in water, is attracted towards the propagation axis of the ray by the gradient force and pushed forward by the scattering force. Particles with refractive index lower that the surrounding medium, for example an air bubble in water, are pushed away from the ray by the gradient force, as shown in Fig. 2.8b. The time scales shown in Fig. 2.8 are obtained by considering the overdamped motion of the particle in the viscous medium, i.e., water, as discussed in detail in Chapter 7.

For particles with high refractive index, one possible approach to achieving a stable trap is to use a second counter-propagating light ray, as shown in Fig. 2.8c. In fact, such

https://doi.org/10.1017/CBO9781107279711.004 Published online by Cambridge University Press

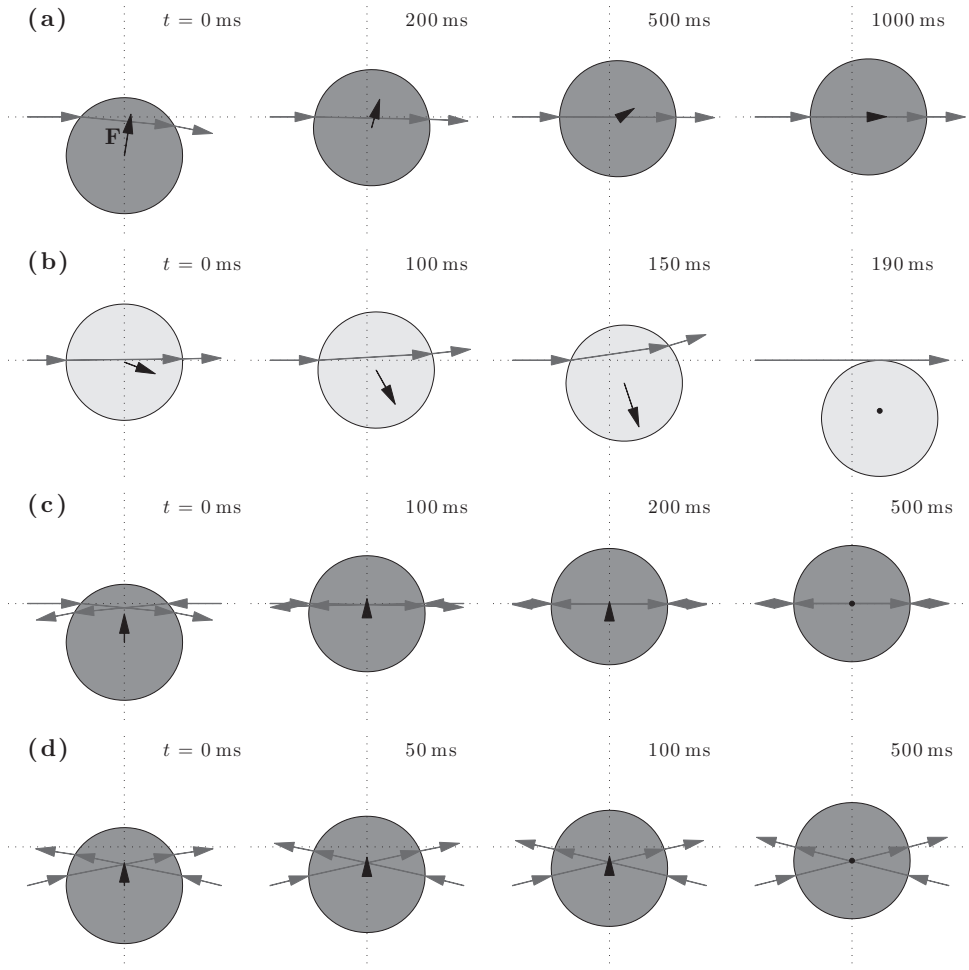

Figure 2.8 Counter-propagating optical tweezers. (a) A glass (radius $a = 3\ \mu\text{m}$, $n_\text{p} = 1.50$) sphere immersed in water ($n_\text{m} = 1.33$) and illuminated by a light ray is attracted towards the ray by the gradient force and pushed forward by the scattering force. (b) An air bubble ($a = 3\ \mu\text{m}$, $n_\text{m} = 1.00$) in water is pushed away from the ray. (c) The addition of a second counter-propagating ray manages to stabilise the glass sphere position. (d) Two counter-propagating rays at an angle generate a stable trapping position towards which the glass sphere is attracted. The black arrows represent the forces. In all cases, only the deterministic optical forces are taken into account; the Brownian motion of the particles is neglected. The times correspond to the overdamped motion of the particle in the viscous medium (see details in Chapter 7).

a configuration using two laser beams was among the first to be employed to trap and manipulate microscopic particles, and a modern version has been obtained using the light emerging from two optical fibres facing each other, as we will see in Section 12.3. This approach also works if the two beams are not perfectly counter-propagating, but are arranged with a sufficiently large angle, as shown in Figs. 2.8d and 2.9a. If the angle between the two

https://doi.org/10.1017/CBO9781107279711.004 Published online by Cambridge University Press

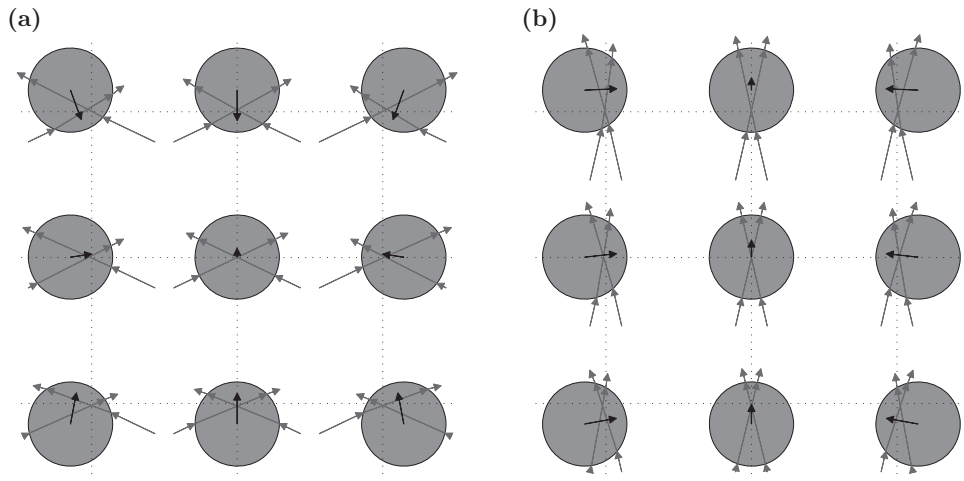

Figure 2.9 Optical trapping by two rays. Optical forces produced by two light rays impinging on a glass ($n_{\mathrm{p}} = 1.50$) sphere immersed in water ($n_{\mathrm{m}} = 1.33$) when they are arranged (a) with a large angle and (b) with a small angle. Only in the first case is there a stable optical trapping position.

rays is not large enough, however, the scattering force prevails and again there is no stable trapping position, as shown in Fig. 2.9b.

Exercise 2.4.1 Study how the trapping of a particle by two counter-propagating rays varies as a function of the particle and medium refractive indices and of the angle between the two rays. What happens when the refractive index of the particle grows? At what angle is trapping lost? [Hint: You can use the program `cptrap` from the book website.]

Exercise 2.4.2 What configuration of rays can be used to trap a particle with refractive index lower than its surrounding medium? Verify your guess numerically. [Hint: You can adapt the program `cptrap` from the book website.]

2.5 Optical tweezers

A more convenient alternative to using several counter-propagating light beams is to use a single highly focused light beam. In fact, rays originating from diametrically opposite points of a high-numerical-aperture (high-NA) focusing lens produce in practice a set of rays that converge at very large angles.

As shown in Fig. 2.10 and explained in detail in Chapter 4, a paraxial light beam can be decomposed into a set of rays $\{\mathbf{r}_{\mathrm{p}}^{(m)}\}$ parallel to the optical axis (z), each with appropriate intensity and polarisation. Focusing is then achieved by an objective lens, which has the effect of bending the light rays towards the focal point **O**, obtaining the set of focused rays $\{\mathbf{r}_{\mathrm{f}}^{(m)}\}$. With an ideal aplanatic lens all the rays are made to converge to **O** (this is the

https://doi.org/10.1017/CBO9781107279711.004 Published online by Cambridge University Press

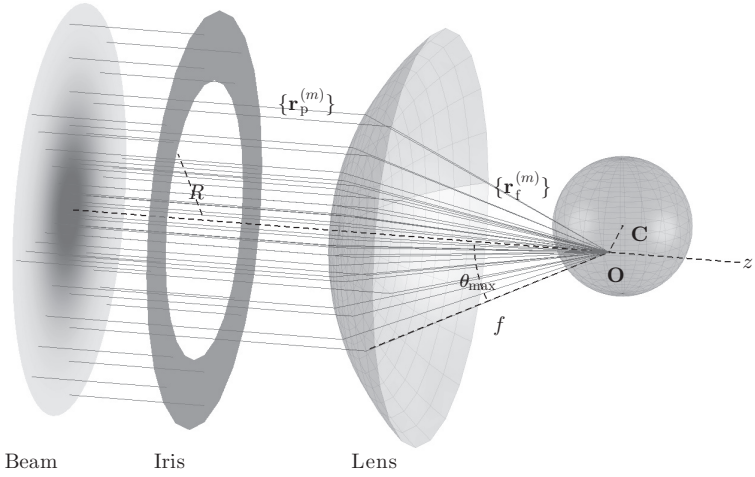

Figure 2.10 Focusing a paraxial light beam. A paraxial light beam is split into a set of parallel light rays $\{\mathbf{r}_{\mathrm{p}}^{(m)}\}$. The focusing objective includes an aperture stop, or iris, with radius R and a focusing lens with focal length f, which bends the rays towards the focus $\mathbf{O}$, obtaining the set of rays $\{\mathbf{r}_{\mathrm{f}}^{(m)}\}$. Here, we have a perfect focus without aberrations; i.e., all rays converge to $\mathbf{O}$. The scattering of $\{\mathbf{r}_{\mathrm{f}}^{(m)}\}$ produces a force $\mathbf{F}_{\mathrm{GO}}$ on the sphere whose centre is placed at $\mathbf{C}$. The NA is related to the angle θ_{max} over which the rays are focused [Eq. (2.22)].

case shown in Fig. 2.10); however, in practice, often there are aberrations [Box 2.2], which decrease the quality of the focus.

To calculate the optical forces, each ray, $\mathbf{r}_{\mathrm{f}}^{(m)}$, is made to interact with a dielectric sphere placed at point $\mathbf{C} = [x, y, z]$ near $\mathbf{O}$ and the resulting force $\mathbf{F}_{\mathrm{ray}}^{(m)}$ is calculated according to Eq. (2.15). Finally, all the forces $\mathbf{F}_{\mathrm{ray}}^{(m)}$ are summed up to obtain the force acting on the centre of mass of the sphere:

$$\mathbf{F}_{\mathrm{GO}} = \sum_m \mathbf{F}_{\mathrm{ray}}^{(m)} = \sum_m \left[\frac{n_{\mathrm{i}} P_{\mathrm{i}}^{(m)}}{c} \hat{\mathbf{r}}_{\mathrm{i}}^{(m)} - \frac{n_{\mathrm{i}} P_{\mathrm{r}}^{(m)}}{c} \hat{\mathbf{r}}_{\mathrm{r},0}^{(m)} - \sum_{n=1}^{+\infty} \frac{n_{\mathrm{i}} P_{\mathrm{t},n}^{(m)}}{c} \hat{\mathbf{r}}_{\mathrm{t},n}^{(m)} \right]. \quad (2.20)$$

As shown in Fig. 2.11, when the object is displaced from its equilibrium position, $\mathbf{C}_{\mathrm{eq}} = [x_{\mathrm{eq}}, y_{\mathrm{eq}}, z_{\mathrm{eq}}]$, which in general does not coincide with $\mathbf{O}$ due to the scattering force, it experiences a *restoring force* proportional to the displacement, at least for relatively small displacements (about up to the particle radius); i.e.,

$$\begin{cases} F_{\mathrm{GO},x} \approx -\kappa_x (x - x_{\mathrm{eq}}), \\ F_{\mathrm{GO},y} \approx -\kappa_y (y - y_{\mathrm{eq}}), \\ F_{\mathrm{GO},z} \approx -\kappa_z (z - z_{\mathrm{eq}}), \end{cases} \quad (2.21)$$

where κ_x, κ_y and κ_z are the spring constants or *trap stiffnesses*. Under the assumption that the beam is circularly polarised, as in Fig. 2.11, the spring constants κ_x and κ_y in the plane perpendicular to the optical axis are exactly equal because the optical forces are rotationally symmetric around the optical axis, whereas the spring constant κ_z in the axial direction is

https://doi.org/10.1017/CBO9781107279711.004 Published online by Cambridge University Press

Box 2.2 Optical aberrations

Chromatic aberrations occur when the refractive index of a material depends on the wavelength (*dispersion*) so that a lens focuses different colours at different focal points. For materials with *normal dispersion*, the refractive index decreases with increasing wavelength, so that longer wavelengths have longer focal lengths. Chromatic aberration can be reduced by increasing the focal length of the lens or by using an achromatic lens (*achromat*), where materials with differing dispersion are assembled together to form a compound lens. Also, many types of glass have been developed to reduce chromatic aberration, such as glasses containing fluorite, which are often employed in the realisation of commercial microscope objectives [Subsection 8.2.1].

Spherical aberrations occur when the light rays that strike a lens near its edge are deflected differently than those that strike the lens nearer the centre. A *positive* (*negative*) *spherical aberration* occurs when peripheral rays are bent too much (are not bent enough).

The *coma*, or *comatic aberration*, is a variation in magnification over the entrance pupil, so that the image of an off-axis object is flared like a comet, hence the name.

The *astigmatism* is due to the fact that rays that propagate in two perpendicular planes have different foci, which are in fact *line foci*, inclined in orthogonal directions and separated by some axial distance.

The *Petzval field curvature*, or *field distortion*, is the optical aberration in which a flat object normal to the optical axis cannot be brought into focus on a flat image plane.

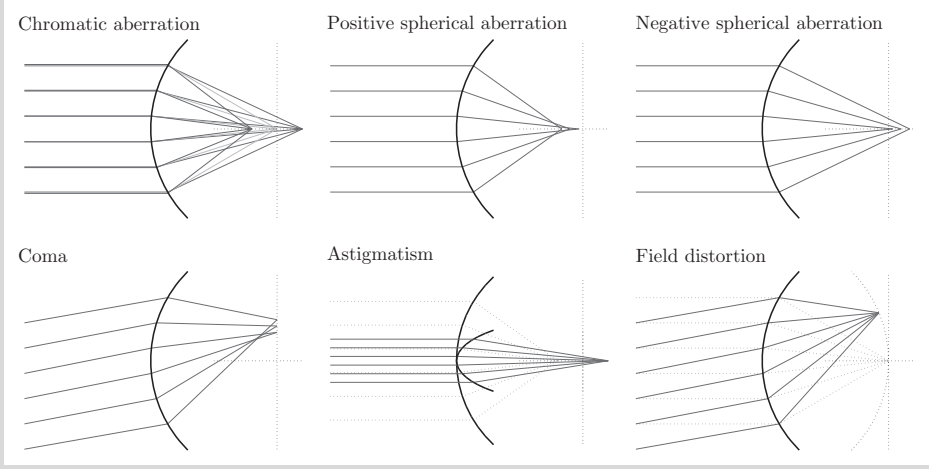

typically smaller. Whereas $\mathbf{F}_{\mathrm{GO}}$ is independent of the particle radius, the stiffness, which is given by the force divided by the displacement, is inversely proportional to the particle size. If the beam is not circularly polarised, the optical forces can become significantly asymmetric; this effect is particularly important for particles whose dimensions are smaller than or similar to the light wavelength, which will be discussed in detail in Chapters 3, 5 and 6.

In Fig. 2.11a, the axial trapping efficiencies are plotted as a function of the particle displacement along the optical axis z ($x = y = 0$), where, because of symmetry, only the longitudinal components are different from zero. Whereas the longitudinal gradient efficiency $Q_{\mathrm{GO,g},z}$ (dashed line) reverses its sign around the focal point $z = 0$, the scattering

https://doi.org/10.1017/CBO9781107279711.004 Published online by Cambridge University Press

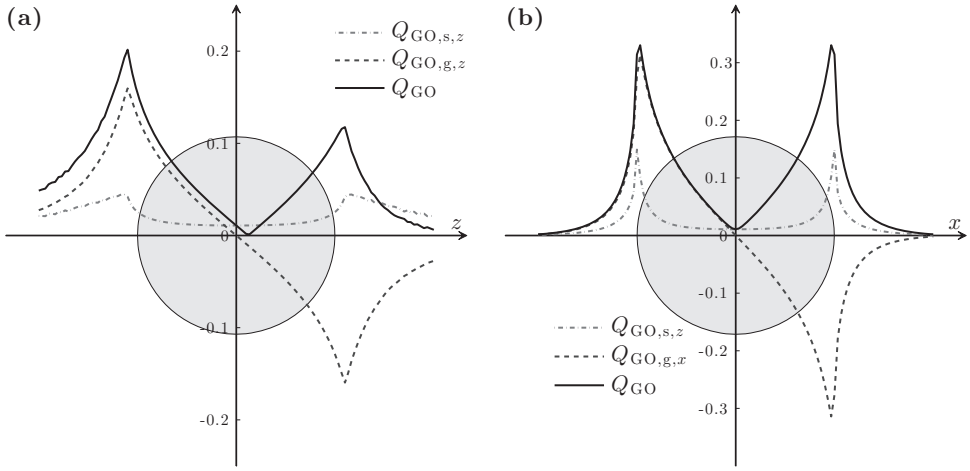

Figure 2.11 Optical trap stiffness. Trapping efficiencies for a glass (radius $a = 3\ \mu\mathrm{m}$, $n_\mathrm{p} = 1.50$) sphere immersed in water ($n_\mathrm{m} = 1.33$) as a function of the particle displacement (a) along the optical axis z ($x = y = 0$), where both the gradient and the scattering forces are aligned along the z-axis, and (b) along the transverse axis x ($y = z = 0$), where the gradient force is aligned along the x-axis and the scattering force is aligned along the z-axis. The focus is obtained by overfilling a water-immersion objective ($\mathrm{NA} = 1.20$).

efficiency $Q_{\mathrm{GO,s},z}$ (dashed-dotted line) is always positive. This scattering force is the reason that the particle equilibrium position in the trap lies just after (not exactly at) the focal point. In Fig. 2.11b, the trapping efficiencies are plotted as a function of the particle displacement along the transverse axis x ($y = z = 0$). In this case, the gradient efficiency has only the x-component, which pulls the particle towards $x = 0$, whereas the scattering efficiency has only the z-component, which pushes the particle along the optical axis. For both longitudinal and transverse displacements, the maximum restoring force is achieved at a displacement of approximately one particle radius.

Exercise 2.5.1 How does the polarisation of the incoming beam affect the trap stiffnesses along the longitudinal and transverse directions? Show that for non-circularly-polarised beams κ_x is generally different from κ_y. [Hint: You can adapt the program `otgo` from the book website.]

Exercise 2.5.2 Show that, in the geometrical optics approximation, the trap stiffness is inversely proportional to the particle radius. [Hint: You can adapt the program `otgo` from the book website.]

Exercise 2.5.3 How do aberrations [Box 2.2] affect the trapping efficiencies? [Hint: You can adapt the program `otgo` from the book website.]

2.6 Filling factor and numerical aperture

The angle θ_max [Fig. 2.10] over which the rays are focused determines the trapping characteristics of the focus and depends both on the radius R of the aperture stop, or iris, and

https://doi.org/10.1017/CBO9781107279711.004 Published online by Cambridge University Press

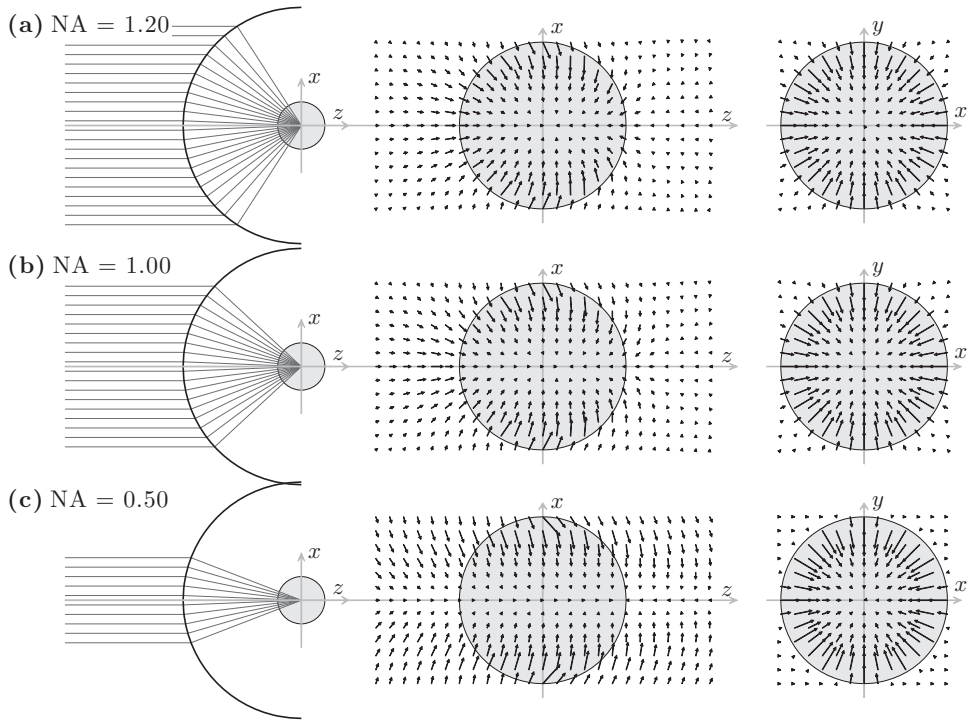

Figure 2.12 Dependence of optical forces on numerical aperture. Optical forces in the longitudinal (zx) and transverse (xy) planes as a function of the NA produced by a focused circularly polarised light beam on a glass (radius $a = 3$ μm, $n_{\mathrm{p}} = 1.50$) sphere immersed in water ($n_{\mathrm{m}} = 1.33$). As the NA decreases, the trapping in the longitudinal plane is lost due to the overwhelming presence of scattering forces. In the transverse plane, trapping is also possible at low NA because it is mainly due to gradient forces.

on the focal length f of the objective lens. A useful parameter that is often employed to characterise θ_{max} is the NA of the objective,

$$\mathrm{NA} = n_{\mathrm{m}} \sin(\theta_{\mathrm{max}}) = n_{\mathrm{m}} \frac{R}{f}, \tag{2.22}$$

where n_{m} is the refractive index of the medium where the light is focused. In Fig. 2.12, the optical forces on a sphere are presented as a function of the NA. For high NA (Fig. 2.12a, NA $= 1.20$ in water), there is a stable trapping position both in the longitudinal plane (zx, containing the optical axis) and in the transverse plane (xy, perpendicular to the optical axis). For lower NA (Figs. 2.12b and 2.12c, NA $= 1.00$ and 0.50, respectively, in water), the particle is still trapped in the transverse plane because of the gradient forces attracting it towards the beam axis, but it is no longer confined along the longitudinal direction. This is in agreement with the fact that, in the presence of only two rays, there is stable trapping only if they are highly convergent, as shown in Fig. 2.9.

Exercise 2.6.1 What is the minimum NA required to trap a glass ($n_{\mathrm{p}} = 1.50$) spherical particle of radius 3 μm in water ($n_{\mathrm{m}} = 1.33$)? How does the minimum NA depend on the

https://doi.org/10.1017/CBO9781107279711.004 Published online by Cambridge University Press

material of the particle, e.g., silica ($n_\mathrm{p} = 1.42$), polystyrene ($n_\mathrm{p} = 1.49$), melamine ($n_\mathrm{p} = 1.60$) and air ($n_\mathrm{p} = 1.00$)? and on the medium, e.g., air ($n_\mathrm{m} = 1.00$) and immersion oil ($n_\mathrm{m} = 1.50$)? [Hint: You can adapt the program `otgo` from the book website.]

2.7 Non-uniform beams

As we have seen in Fig. 2.7, the parts of the beam that contribute most to the trapping efficiencies are the rays propagating with very large angles originating from the edge of the aperture. Therefore, it is reasonable to consider whether beams that do not fill the objective aperture uniformly could be more efficient at achieving stable trapping. We consider some such cases in Fig. 2.13. Fig. 2.13a shows the trapping efficiencies for a Gaussian beam with a waist equal to 30% of the objective pupil (NA = 1.20 in water): although gradient forces ($\propto Q_{\mathrm{GO,g},x}$) allow effective trapping in the transverse plane, the push of the scattering forces

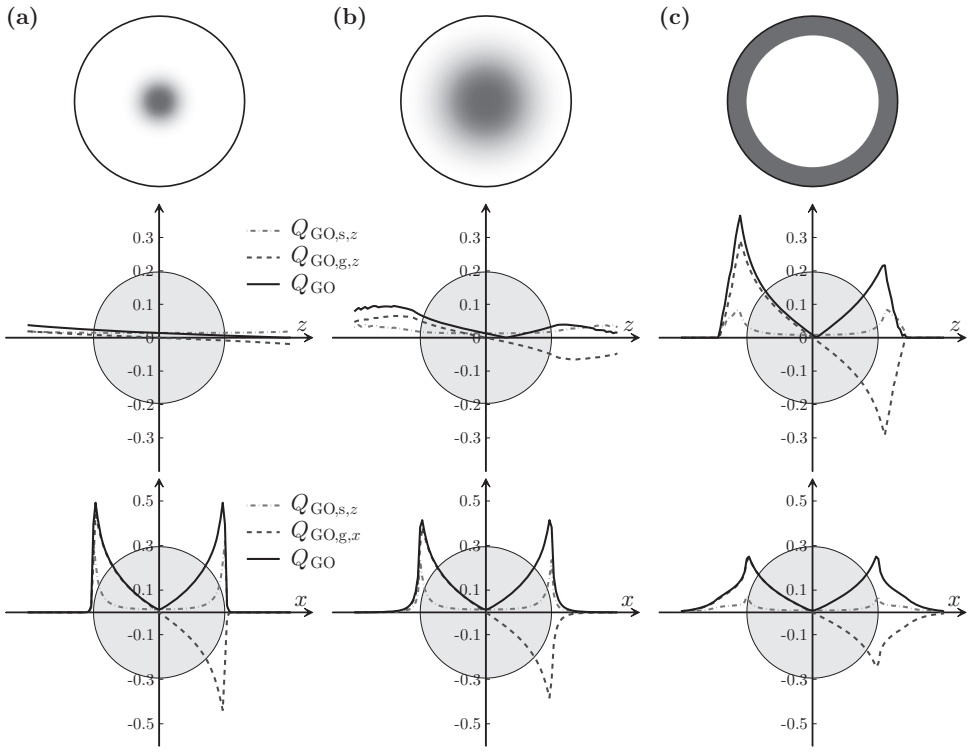

Figure 2.13 Optical traps with non-uniform beams. Trapping efficiencies in the longitudinal (top) and transverse (bottom) planes for a Gaussian beam with waist equal to (a) 30% and (b) 70% of the objective pupil aperture, and (c) for an annular beam. We consider the trapping of a glass (radius $a = 3\ \mu\mathrm{m}$, $n_\mathrm{p} = 1.50$) sphere immersed in water ($n_\mathrm{m} = 1.33$). The beam profile on the water-immersion objective (NA = 1.20) entrance pupil is shown at the top.

https://doi.org/10.1017/CBO9781107279711.004 Published online by Cambridge University Press

($\propto Q_{\mathrm{GO,s},z}$) does not permit effective trapping of the particle along the optical axis. When the waist of the beam is increased to 70% of the objective pupil, as shown in Fig. 2.13b, a longitudinal gradient force ($\propto Q_{\mathrm{GO,g},z}$) large enough to overcome the scattering force along z ($\propto Q_{\mathrm{GO,s},z}$) arises. In fact, as the objective *filling factor* increases, more rays are present at a high angle, where they contribute most to the trapping efficiencies, so that the axial trapping efficiency increases. As we will see in the experimental part of this book, this is the reason that overfilling of the objective aperture is typically a requirement to obtain a stable optical trap, even though it reduces the power available for trapping, as the tails of the Gaussian are cut off by the iris.

Building on the observations made in the previous paragraph, we might consider using an annular beam, i.e., a beam with an annular distribution of light intensity, to enhance axial trapping, as shown in Fig. 2.13c. We note that in this discussion we have not considered the phase of the beam. In fact, as will be discussed in Chapter 4, many beams with a complex intensity profile, e.g., Laguerre–Gaussian beams [Subsection 4.4.3], Bessel beams [Subsection 4.4.4] and cylindrical vector beams [Subsection 4.4.5], also present a complex phase and/or polarisation profile that can have major effects on their trapping properties. In fact, some of the aspects that cannot be easily modelled within the geometrical optics approach are the features related to the presence of spin angular momentum (SAM) and of a nonuniform phase profile, which lead, e.g., to the presence of orbital angular momentum (OAM). The discussion of the mechanical effects of non-Gaussian beams, OAM and SAM will be developed in detail in Chapters 3, 5 and 6 within the electromagnetic theory description of optical forces and torques.

Exercise 2.7.1 What is the optimal beam profile to achieve the highest longitudinal trapping efficiency for a glass ($n_{\mathrm{p}} = 1.50$) particle of radius 3 μm in water ($n_{\mathrm{m}} = 1.33$)? What is the optimal beam profile to obtain the highest transverse trapping efficiency? Use a water-immersion objective with NA $= 1.20$. Note that they are not the same. Why? [Hint: You can use the program `otgo` from the book website.]

Exercise 2.7.2 Calculate the optical forces on an air bubble immersed in oil. Show that there is no stable equilibrium position when a single Gaussian beam is used, whereas it is possible to trap the bubble stably using an annular beam. What happens when two counter-propagating beams are employed? [Hint: You can use the program `otgo` from the book website.]

2.8 Non-spherical objects and the windmill effect

A geometrical optics approach similar to the one we followed in the derivation of the forces acting on a microscopic sphere can be employed to study more complex geometries, as long as all the characteristic dimensions of the object under study are significantly larger than the wavelength of the light used for trapping. A simple case is that of a cylindrical object, such as the one shown in Fig. 2.14a. The basic interaction of a ray with the cylinder is the same as for the sphere and the force can be calculated using the formula in Eq. (2.20).

https://doi.org/10.1017/CBO9781107279711.004 Published online by Cambridge University Press

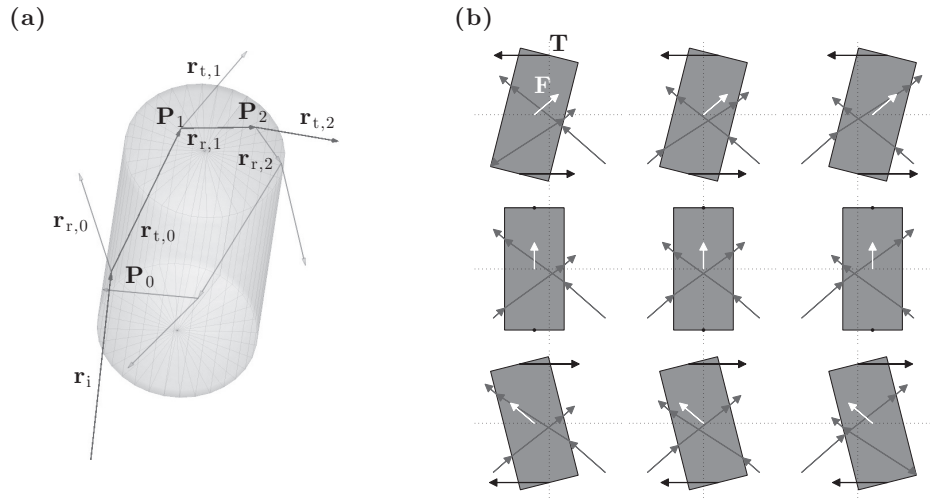

Figure 2.14 Optical force and torque on a cylinder. (a) Multiple scattering of a light ray impinging on a cylinder visualised in three dimensions. Note that, differently from the case of a sphere [Fig. 2.6], the reflected and transmitted rays are not all on the same plane. (b) Optical forces (white arrows) and torques (black arrows) produced by two light rays impinging on a cylinder at a large angle. The torque tends to align the cylinder along the optical axis. In all cases, there is a scattering force pushing the cylinder along the optical axis.

There are two major differences, though. The first is that in the case of nonspherical objects a significant torque can also appear. The torque due to a single ray can be calculated as the difference of the angular momentum associated with the incoming ray and that of the outgoing rays, i.e.,

$$\mathbf{T}_{\text{ray}}^{(m)} = (\mathbf{P}_0 - \mathbf{C}) \times \frac{n_\text{i} P_\text{i}^{(m)}}{c} \hat{\mathbf{r}}_\text{i}^{(m)} - (\mathbf{P}_0 - \mathbf{C}) \times \frac{n_\text{i} P_\text{r}^{(m)}}{c} \hat{\mathbf{r}}_{\text{r},0}^{(m)} - \sum_{n=1}^{+\infty} (\mathbf{P}_n - \mathbf{C}) \times \frac{n_\text{i} P_{\text{t},n}^{(m)}}{c} \hat{\mathbf{r}}_{\text{t},n}^{(m)}, \tag{2.23}$$

where $\mathbf{C}$ is the centre of mass of the object, $\mathbf{P}_0$ is the incidence point of the incoming ray and $\{\mathbf{P}_n\}$ are the scattering points of the subsequently scattered rays. Then the total torque on the object can be calculated as the sum of the torques due to each ray:

$$\mathbf{T}_{\text{GO}} = \sum_m \mathbf{T}_{\text{ray}}^{(m)}. \tag{2.24}$$

The black arrows in Fig. 2.14b show the torque arising on a cylinder due to a pair of rays. This torque tends to align the cylinder along the optical axis.

The second difference is that for a spherical particle the radiation pressure of a plane wave, i.e., a set of parallel rays, is always directed in the propagation direction because of symmetry. However, for anisotropic shapes the radiation pressure has a transverse

https://doi.org/10.1017/CBO9781107279711.004 Published online by Cambridge University Press

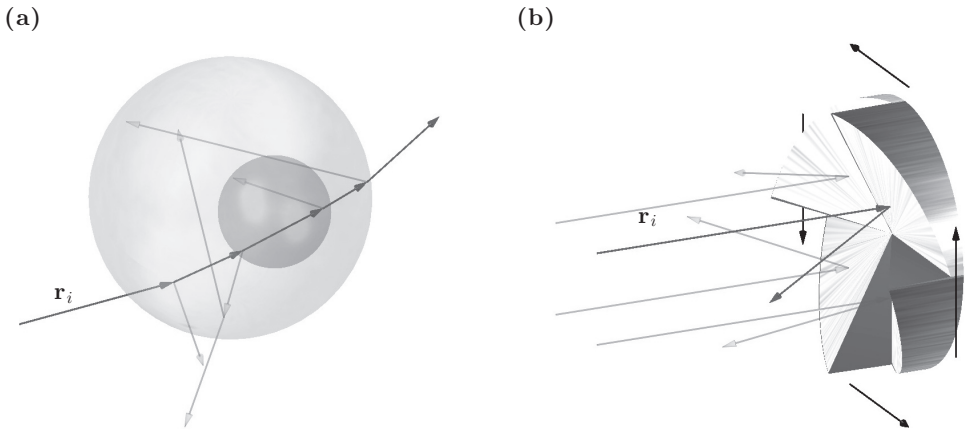

Figure 2.15 Trapping non-convex shapes and the windmill effect. (a) Multiple scattering of a ray on a complex shape constituted by two spheres, one inside the other; this is a simple optical model for a cell containing a nucleus. (b) The asymmetric deflection of the incoming rays on a non-cylindrically-symmetric object produces the torque indicated by the black arrows and the rotation of the object. This phenomenon is known as the *windmill effect*.

component that is responsible for the *optical lift effect*; i.e., non-spherical particles can move transversely to the incident light propagation direction.

More complex objects can be modelled by more complex shapes. For example, as a first approximation, a cell containing a nucleus can be modelled by a sphere (the cytoplasm) containing a smaller sphere of different refractive index (the nucleus), as shown in Fig. 2.15a. It is interesting to notice that in a scattering event a ray can now be split into multiple rays that may not necessarily be able to escape the particle; this is typical of all nonconvex shapes and can lead to an explosion in the number of rays to be taken into account.

In the presence of an optical torque, the object rotates in a certain direction. This effect is known as the *windmill effect* because of its analogy to the motion of a windmill, where the wind in this case is the flow of momentum due to the electromagnetic field, as shown in Fig. 2.15b. This effect should not be confused with the rotation induced by the transfer of SAM and OAM, which will be described in detail in Chapters 5 and 6.

Exercise 2.8.1 A ray scattering on a sphere does not produce any torque on the sphere itself. Verify this fact with some numerical simulations and demonstrate it analytically. Conclude that a beam also cannot produce any torque on a sphere.

Exercise 2.8.2 What are the forces and torques acting on a cylinder illuminated by a plane wave?

Exercise 2.8.3 Calculate the optical forces and torques acting on an object such as the one shown in Fig. 2.15a.

Exercise 2.8.4 Calculate the optical windmill effect on an object such as the one shown in Fig. 2.15b.

https://doi.org/10.1017/CBO9781107279711.004 Published online by Cambridge University Press

Problems

2.1 Given a light beam propagating in the positive z-direction and linearly polarised along the x-direction, calculate numerically the optical trapping efficiencies in the case of a sphere. What do you observe? How do your results compare with the ones presented in the text for the case of a circularly polarised beam?

2.2 Calculate the optical forces and torques acting on an ellipsoid with semi-axes $a_1, a_2, a_3 \gg \lambda_0$ held in an optical tweezers. What is the ellipsoidal equilibrium configuration for the three cases $a_1 > a_2 > a_3$, $a_1 > a_2 = a_3$ (prolate spheroid), and $a_1 = a_2 > a_3$ (oblate spheroid)? How does the force scale with the ratio a_1/a_3 in the case of spheroids?

2.3 Consider a circularly polarised light beam that is reflected by a mirror. Knowing that the spin of a photon is $\hbar$, calculate the optical torque transferred to the mirror upon reflection. What happens if the beam is completely absorbed by the object? What is the maximum torque that can be exerted on the mirror? What are the limits of geometrical optics in the description of this phenomenon?

2.4 Calculate the optical forces arising on a human red blood cell, whose shape is a biconcave disc because of the absence of the nucleus.

2.5 Calculate the optically induced stress profile over the surface of a microscopic bubble. Evaluate also the resulting deformation using elastic membrane theory, e.g., following the approach used by Skelton et al. (2012).

2.6 *Trapping through an interface.* In a standard optical tweezers, the beam is often focused through a planar interface that presents a refractive index mismatch (e.g., between the coverslip glass and the sample water). What kind of aberrations does this introduce? How does the focal point change? How does this affect the optical forces on a spherical particle? How does this depend on the distance between the focal point and the planar interface?

2.7 *Optical binding.* Consider a spherical particle under plane wave illumination. This particle acts as a lens focusing the light beam. Now, consider a second particle placed near the resulting focus. What kind of optical forces does this second particle experience? What happens if the two particles are placed between two counter-propagating plane waves?

2.8 *Layered spheres.* Consider a dielectric layered sphere, constituted by a core covered by a multilayer. Such a model was employed by Chang et al. (2006) to describe the optical properties of a cell. Calculate the resulting optical forces using ray optics under various illumination conditions.

2.9 *Janus particles.* Consider a Janus sphere, i.e., a particle whose hemispheres have different refractive indices. Calculate the optical forces and torques on such objects

https://doi.org/10.1017/CBO9781107279711.004 Published online by Cambridge University Press

using ray optics. How does this particle align in an optical tweezers? What happens if the particle has a cylindrical or ellipsoidal shape?

2.10 *Absorbing and reflecting objects.* Consider a sphere made of an absorbing material. What optical forces and torques can a single ray produce on such a sphere? What happens for a focused beam? Under what conditions is it possible to trap it? Repeat the same analysis for the case of a reflecting sphere.

2.11 *Metamaterials.* Metamaterials are artificial materials engineered to have properties that may not be found in nature. For example, it might be possible to have some materials with negative refractive index. Study the optical forces that might arise on a particle made of such a material.

References

Abraham, M. 1909. Zur Elektrodynamik bewegter Körper. *R. C. Circ. Mat. Palermo*, 1–28.

Ashkin, A. 1992. Forces of a single-beam gradient laser trap on a dielectric sphere in the ray optics regime. *Biophys. J.*, **61**, 569–82.

Ashkin, A., and Dziedzic, J. M. 1973. Radiation pressure on a free liquid surface. *Phys. Rev. Lett.*, **30**, 139–42.

Barnett, S. M. 2010. Resolution of the Abraham–Minkowski dilemma. *Phys. Rev. Lett.*, **104**, 070401.

Chang, Y.-R., Hsu, L., and Chi, S. 2006. Optical trapping of a spherically symmetric sphere in the ray-optics regime: A model for optical tweezers upon cells. *Appl. Opt.*, **45**, 3885–92.

Minkowski, H. 1908. Die Grundgleichungen für die elektromagnetischen Vorgänge in bewegten Körpern. *Nachr. Ges. Wiss. Göttingen*, 53–111.

Pfeifer, R. N. C., Nieminen, T. A., Heckenberg, N. R., and Rubinsztein-Dunlop, H. 2007. Momentum of an electromagnetic wave in dielectric media. *Rev. Mod. Phys.*, **79**, 1197–1216.

Skelton, S. E., Sergides, M., Memoli, G., Maragò, O. M., and Jones, P. H. 2012. Trapping and deformation of microbubbles in a dual-beam fibre-optic trap. *J. Opt.*, **14**, 075706.

https://doi.org/10.1017/CBO9781107279711.004 Published online by Cambridge University Press